Functionalized Organosilica Microspheres via a Novel Emulsion-Based Route

Chris R. Miller, Robert Vogel, Peter P. T. Surawski, Kevin S. Jack, Simon R. Corrie, and Matt Trau*

Centre for Nanotechnology and Biomaterials, Department of Chemistry, The University of Queensland, St. Lucia QLD 4072, Australia

Received May 29, 2005. In Final Form: August 1, 2005

Thiol-functionalized organosilica microspheres were synthesized via a two-step process: (1) acid-catalyzed hydrolysis and condensation of 3-mercaptopropyltrimethoxysilane (MPTMS), followed by (2) base-catalyzed condensation, which led to the rapid formation of emulsion droplets with a narrow size distribution. These droplets continued to condense to form solid microspheres. Solution ^{29}Si NMR and optical microscopy were applied to study the mechanism of this novel synthetic route. Solid-state ^{29}Si NMR, SEM, zeta potential titration, and Coulter counter measurements were used to study the bulk and surface properties and to determine the particle size distributions of the final microspheres. Compared to conventional Stöber silica particles, these microspheres were shown to have a lower degree of cross-linking (average degree of condensation, $r = 1.25$), a larger average size (up to 6 μm), and a higher isoelectric point (pH = 4.4). Confocal microscopy of dye-labeled microspheres showed an even distribution of dye molecules throughout the interior, characteristic of a readily accessible and permeable organosilica network. These findings have implications for the production of functionalized solid supports for use in catalysis and biological applications, such as optically encoded carriers for combinatorial synthesis.

1. Introduction

There has been increased interest in the synthesis of silica microspheres in the last few decades due to their many scientific and industrial applications. Silica microspheres that are uniform in size, shape, and composition have been used as model systems to study fundamental physical chemistry processes, e.g., light scattering, colloidal stability, and rheology, as well as in important industrial applications, such as catalysts, ceramics, pigments, immunoassays, etc.[1] The preparation of mesoporous silica microspheres has an equally wide range of applications including selective adsorption, chemical sensing, chromatography, and as a controlled-release drug delivery platform.[2,3]

An emerging area of application for functionalized organosilica microspheres is their use as optically encoded carriers in the combinatorial synthesis of oligonucleotide and peptide libraries.[4,5] The desired size range of such microspheres is currently thought to be between 5 and 15 μm for compatibility with high-throughput detection techniques such as flow cytometry.[6,7]

A well-known method for the preparation of uniform micrometer-sized silica microspheres was developed by Stöber et al.,[8] involving the hydrolysis and condensation of tetraethyl orthosilicate (TEOS) in an alcohol/water mixture using ammonia as a base catalyst. The maximum particle size via a one-step Stöber synthesis while still maintaining monodispersity is 1.9 μm in diameter.[9,10] With the use of a seeded growth technique,[1] it is possible to achieve both a larger size (up to 3.6 μm) and a larger mass fraction (up to 10%) by reacting additional TEOS and H_2O with an initial seed suspension of microspheres generated by the above method.

A useful application of the seeded growth (or core/shell) technique is the introduction of organic species into the shell layers. In this manner, microspheres may be surface-modified with, e.g., amine groups,[11] through the hydrolysis and condensation of the appropriate organosilane. Alternatively, an organic dye may be incorporated in the shell layer via entrapment,[12] or in the case of amine-reactive dyes, by covalent attachment to 3-aminopropyltriethoxysilane (APS).[11] This concept may even be extended to multiple shell layers, each containing a different organic dye.[13]

While the above methods are capable of producing silica microspheres of a narrow size distribution with a variety of different functional groups, they are limited to microspheres less than 5 μm in size. One approach to synthesizing larger silica microspheres involves mechanical means to generate large droplets of monomer solution which then gel upon exposure to basic catalysts to form solid microspheres. A variety of techniques have been attempted, including aerospray (10−20 μm),[14] micrometer-sized injection nozzles (1−200 μm),[15] and ultrasonic

* Corresponding author. Phone: + 61 7 3365 3816. Fax: + 61 7 3365 4299. E-mail: m.trau@uq.edu.au.

(1) Giesche, H. *J. Eur. Ceram. Soc.* **1994**, *14*, 205.
(2) Chevalier, P. M.; Ou, D. L. *J. Mater. Chem.* **2002**, *12*, 3003.
(3) Walcarius, A.; Delacote, C. *Chem. Mater.* **2003**, *15*, 4181.
(4) Gunderson, K. L.; Kruglyak, S.; Graige, M. S.; Garcia, F.; Kermani, B. G.; Zhao, C. F.; Che, D. P.; Dickinson, T.; Wickham, E.; Bierle, J.; Doucet, D.; Milewski, M.; Yang, R.; Siegmund, C.; Haas, J.; Zhou, L. X.; Oliphant, A.; Fan, J. B.; Barnard, S.; Chee, M. S. *Genome Res.* **2004**, *14*, 870.
(5) Battersby, B. J.; Lawrie, G. A.; Trau, M. *Drug Discovery Today* **2001**, *6*, S19.
(6) Kellar, K. L.; Oliver, K. G. In *Cytometry, New Developments*, 4th ed.; Darzynkiewicz, Z., Roederer, M., Tanke, H., Eds.; Elsevier Academic: New York, 2004; p 409.
(7) Gao, X. H.; Nie, S. M. *Anal. Chem.* **2004**, *76*, 2406.
(8) Stöber, W.; Fink, A.; Bohn, E. *J. Colloid Interface Sci.* **1968**, *26*, 62.
(9) Tan, C. G.; Bowen, B. D.; Epstein, N. *J. Colloid Interface Sci.* **1987**, *118*, 290.
(10) Bogush, G. H.; Tracy, M. A.; Zukoski, C. F. *J. Non-Cryst. Solids* **1988**, *104*, 95.
(11) van Blaaderen, A.; Vrij, A. *Langmuir* **1992**, *8*, 2921.
(12) Giesche, H.; Matijevic, E. *Dyes Pigm.* **1991**, *17*, 323.
(13) Lawrie, G. A.; Battersby, B. J.; Trau, M. *Adv. Funct. Mater.* **2003**, *13*, 887.
(14) Kortesuo, P.; Ahola, M.; Kangas, M.; Yli-Urpo, A.; Kiesvaara, J.; Marvola, M. *Int. J. Pharm.* **2001**, *221*, 107.

10.1021/la0514112 CCC: $30.25
Published on Web 09/09/2005

oscillation (1−3 μm).[16] A common characteristic of all these methods is a high degree of polydispersity in the size distribution due to the lack of control of size or colloidal stability.

An alternative two-step approach to synthesize suitable microspheres for use as carriers in combinatorial synthesis was developed by Johnston et al.[17,18] In the first step, the hydrolysis and condensation of 3-mercaptopropyltrimethoxysilane (MPTMS) in aqueous HCl solution leads to an insoluble oil phase. In the second step, the oil-in-water emulsion is added to an ammonia solution which cross-links the oil droplets, leading to polydisperse porous organosilica microspheres between 1 and 100 μm in diameter. Barbé et al.[19] take the reverse approach of a water-in-oil emulsion, stabilized by surfactant, to produce homogeneous microspheres of a tunable size range between 50 nm and 50 μm.

In this paper, we describe a novel surfactant-free synthetic route of fabricating functionalized organosilica microspheres via a two-step process which leads to the formation of emulsion droplets with a narrow size distribution. These droplets further condense to form solid microspheres with an equally narrow distribution of particle sizes. This process was characterized using ^{29}Si NMR, SEM, TEM, Coulter counter, and optical microscopy. The proposed mechanism of the formation of the organosilica microspheres differs significantly from the above-mentioned routes in that it shows some analogy to the emulsion polymerization mechanism common to organic polymers.[20]

2. Experimental Section

2.1. Materials. 3-Mercaptopropyltrimethoxysilane (MPTMS, 95%) was obtained from Lancaster and used as supplied. Triethylamine (TEA, 99%), hydrochloric acid (37%), tetrahydrofuran (THF), acetone-d_6 (containing 1% (v/v) tetramethylsilane (TMS)) and AR grade ethanol were all obtained from Sigma-Aldrich. Water was purified using a Millipore Milli-Q filtration system. Rhodamine B isothiocyanate (RBITC) was obtained from Sigma-Aldrich and prepared as a 1×10^{-4} M solution in tetrahydrofuran.

2.2. Synthesis of Organosilica Microspheres. The overall methodology for the synthesis and functionalization of organosilica microspheres is provided in Scheme 1. In a typical experiment (at room temperature, 25 °C), 80 mL of water was placed in a 100 mL Schott bottle stirred at a moderate rate by a Teflon-coated magnetic stirrer. The solution was acidified with 1.6 mL of 0.1 M HCl (pH = 2.7), to which 10 mL of MPTMS was then added. The MPTMS was initially insoluble and formed an emulsion (Scheme 1, E1) that gradually disappeared as the MPTMS hydrolyzed and became more soluble. If left to react under stirring for longer than 8 h, a new emulsion phase appeared (Scheme 1, E2).

Typically, after 18 h, 100 μL of TEA was then rapidly injected into the stirred solution. The initially translucent solution turned cloudy within 30 s and quickly became fully opalescent due to the presence of a new emulsion phase (Scheme 1, E3).

Approximately 30 min after the addition of TEA, the solution was centrifuged at 2000*g* for 5 min. The relatively clear supernatant was discarded leaving a white particulate matter. These particles then underwent a total of three washing cycles consisting of redispersal in ethanol under ultrasonication, followed by centrifugation at 2000*g* for 2 min, to remove the TEA as well as any unreacted monomer or oligomers. The particles thus isolated were easily redispersed by shaking or sonication once transferred into ethanol and freely sedimented leaving a clear solution.

Scheme 1. Overall Methodology for Synthesis of Functionalized Organosilica Microspheres[a]

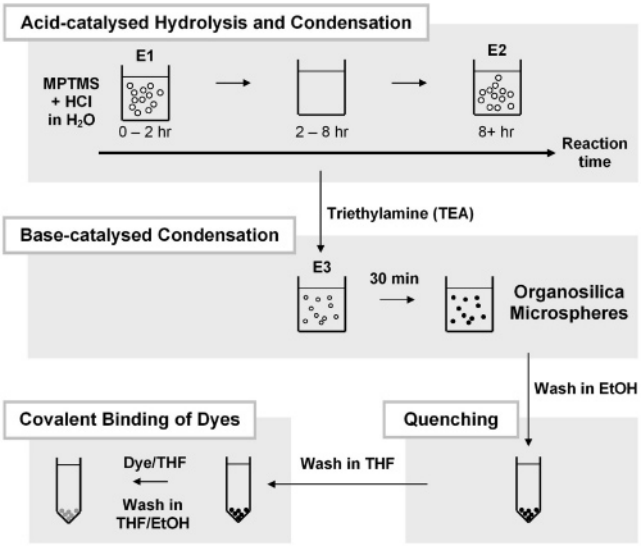

[a] The different emulsion phases formed during synthesis are designated E1−3. The initial E1 phase is consumed during acid-catalyzed hydrolysis, while the E2 phase slowly forms after ~8 h of acid-catalyzed condensation. A base catalyst may be added after 1 h to 2 days of acid-catalyzed hydrolysis and condensation. The E3 phase rapidly forms upon addition of a base catalyst and further condenses to produce solid organosilica microspheres. A typical experiment is described in section 2.2.

2.3. Time Study. To investigate the effect on final particle size due to the length of time spent undergoing acid-catalyzed condensation, microspheres were synthesized as above by adding TEA after various times (between 1 and 48 h) to the precursor solution.

2.4. Covalent Binding of Dyes. Microspheres obtained as above were transferred into THF via multiple washing cycles and subsequently suspended in 100 μL of THF and 20 μL of the 1×10^{-4} M RBITC solution. This mixture was agitated gently for 2 h under dark conditions. The final microsphere pellets were washed once in THF and 4 times in ethanol to remove any excess dye. Samples were stored at 4 °C under dark conditions until examination.

2.5. Nuclear Magnetic Resonance (NMR) Spectroscopy. High-resolution ^{29}Si NMR analysis was performed using a 5 mm broadband probe on a Bruker AV500 NMR spectrometer operating at 99.358 MHz. Aqueous phase and suspension samples (25% v/v) and MPTMS and oil phase samples (10% v/v) were prepared in acetone-d_6 up to a final volume of 1 mL. ^{29}Si spectra were referenced to 1% TMS (0 ppm) added to each sample.

^{29}Si spectra were acquired using the DEPT sequence.[21] The τ delay was set for $^2J_{Si-H}$ equal to 9.5 Hz, and the final proton observation pulse width was optimized for 2-coupled protons. ^{1}H composite pulse decoupling was applied during the acquisition time. For each sample, 160 scans were acquired with a spectral width of 8930 Hz using an acquisition time of 2.5 s and an additional relaxation delay of 15 s. A line-broadening of 0.5 Hz and zero-filling was applied to the spectra before transformation to give a final digital resolution of less than 0.14 Hz.

The ^{29}Si solid-state NMR spectrum was run on a Bruker MSL300 NMR spectrometer operating at 300.13 MHz for ^{1}H and 59.627 MHz for ^{29}Si. Experiments were performed with a standard Bruker 4 mm MAS probe. The MAS spinning speed was 5 kHz. The 90° pulse times for both ^{1}H and ^{29}Si were 5 μs. The spectra were recorded using the standard pulse and collection sequence

(15) Masuda, R.; Takahashi, W.; Ishii, M. *J. Non-Cryst. Solids* **1990**, *121*, 389.
(16) Isobe, H.; Kaneko, K. *J. Colloid Interface Sci.* **1999**, *212*, 234.
(17) Johnston, A. P. R.; Battersby, B. J.; Lawrie, G. A.; Lambert, L. K.; Trau, M. Submitted for publication to *Chem. Mater.*, 2005.
(18) Johnston, A. P. R.; Battersby, B. J.; Lawrie, G. A.; Trau, M. *Chem. Commun.* **2005**, No. 7, 848.
(19) Barbé, C.; Bartlett, J.; Kong, L. G.; Finnie, K.; Lin, H. Q.; Larkin, M.; Calleja, S.; Bush, A.; Calleja, G. *Adv. Mater.* **2004**, *16*, 1959.
(20) Ravve, A. *Principles of Polymer Chemistry*; Kluwer Academic: London, 2000.
(21) Doddrell, D. M.; Pegg, D. T.; Brooks, W.; Bendall, M. R. *J. Am. Chem. Soc.* **1981**, *103*, 727.

with a recycle delay of 100 s and high-power proton decoupling during the acquisition. The spectral width was 29.4 kHz, and over 5000 data points were collected. On processing, a line broadening of 50 Hz was used.

Standard notation for describing different silicate units is used in this paper, i.e., Q_n for quaternary species or T_n for ternary species, where the numerical subscript, n, indicates the number of siloxane bonds involved.

2.6. Optical Microscopy. High-speed photographs (1000 frames per second) of the reaction mixture placed on a microscope slide were obtained with a Phantom v5.0 high-speed camera (Vision Research, Inc.) coupled to an Olympus IX70 optical microscope operating under brightfield conditions at 150× magnification.

2.7. Confocal Microscopy. Fluorescence confocal microscopy images of RBITC-labeled samples were collected using a Zeiss 510 Meta confocal microscope with a HeNe 543 nm laser light source. Samples dried from ethanol were prepared and fixed on a microscope slide and visualized through a 100× oil-immersion objective. Intensity plots were obtained using Image-Pro software (Media Cybernetics).

2.8. Scanning Electron Microscopy (SEM). Uncoated samples (dried at 40 °C onto stubs) were imaged with a JEOL 6460LA scanning electron microscope operating at 10 kV accelerating voltage. The samples were examined at low vacuum (1 Pa) using a solid-state backscattered electron detector operating in COMP (compositional contrast) mode. SEM images of Pt-coated samples were taken with a JEOL 6300 SEM operating at 5 kV accelerating voltage. Images of the Pt-coated samples were analyzed using Image-Pro software to determine size distributions, using a minimum of 800 individual particles per sample.

A high-resolution JEOL 890 microscope was used to provide maximum resolution images of fractured particle surfaces. For sample preparation, particles were transferred into MilliQ water and crushed in a mortar and pestle to expose the internal structures. Holey carbon-coated copper TEM grids were used as the mounting medium, and samples were sputter-coated with platinum. Samples were analyzed using an accelerating voltage of 5 kV and a current of 2×10^{-12}A.

2.9. Zeta Potential Titration Measurements. The zeta potential was measured on a Malvern Instruments Nano ZS Zetasizer, using a flow through cell with a Malvern Instruments MPT-2 Multi Purpose Titrator. Zeta potential measurements were recorded at intervals of approximately 0.5 of a pH unit with 30 runs per pH value.

2.10. Multisizing Measurements (Coulter Counter). Volume-sensing measurements were performed with a Multisizer 3 Coulter counter using a 50 μm nozzle (measured size range: 1−30 μm). Samples were initially dispersed in a 0.1% SDS solution and diluted with a 3% trisodium phosphate solution. Each sample was analyzed for 300 s, with an average detection count in excess of 5×10^5 individual particles per sample.

3. Results and Discussion

3.1. Acid-Catalyzed Hydrolysis and Condensation of MPTMS in Aqueous Solution. The initial acid-catalyzed hydrolysis of MPTMS in aqueous solution was studied using ^{29}Si NMR. MPTMS forms an immiscible phase (E1) in water at the concentrations described above. ^{29}Si NMR spectra of the E1 and aqueous phases after 5 min of acid-catalyzed hydrolysis are compared with MPTMS in Figure 1. Both the MPTMS and E1 phase contain a single peak at −42.57 ppm, confirmed by GC-MS (data not shown) to be the nonhydrolyzed, i.e., fully methoxylated, monomer. This value is consistent with other organotrialkoxysilanes, such as 3-aminopropyl)-triethoxysilane (−44.2 ppm), methyltriethoxysilane (−41.4 ppm), and acrylpropyltrimethoxysilane (−41.8 ppm).[22]

The E1 phase also contained a small peak at −50.78 ppm, attributed to be a dimer by analogy with the $\Delta\delta$ values between monomeric and dimeric species in other alkoxysilanes (i.e., 8−9 ppm upfield).[23] Nonhydrolyzed dimer was identified by GC-MS as an impurity (<1%) in the neat MPTMS and can be formed by the presence of a small amount of water in the sample leading to partial hydrolysis followed by rapid condensation. The absence of this peak in the aqueous phase suggests that the nonhydrolyzed dimer is more soluble in the E1 phase.

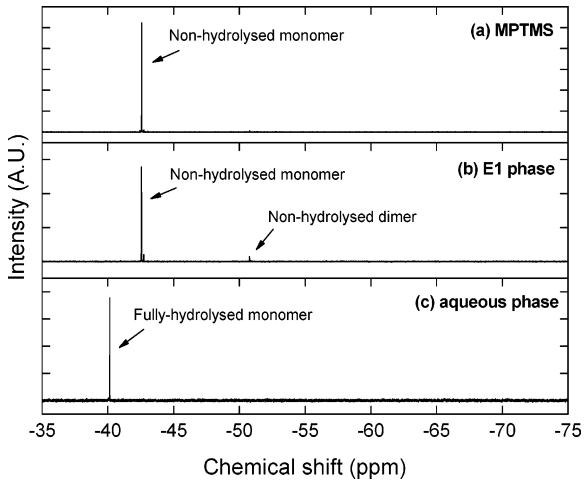

Figure 1. ^{29}Si NMR spectra of (a) initial MPTMS, (b) E1 phase, and (c) aqueous phase following 5 min of acid-catalyzed hydrolysis of MPTMS in aqueous solution. Chemical shifts were adjusted for TMS at 0 ppm.

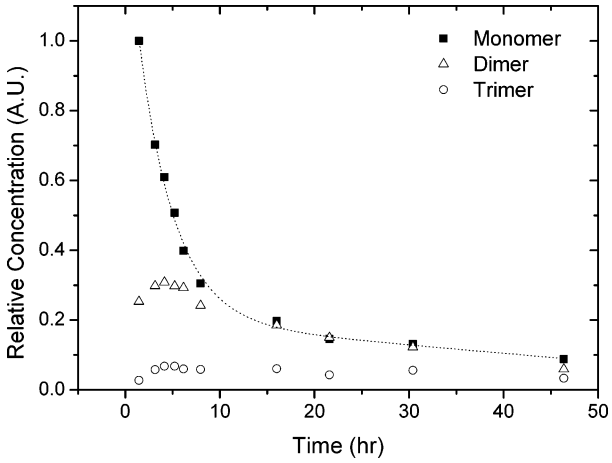

Figure 2. Time evolution of soluble silica species during the acid-catalyzed hydrolysis and condensation of MPTMS. A first-order exponential decay (dotted line) could be fitted to the plot of monomer concentration with time, $k = 4.33$ hr^{-1}. Relative concentrations were calculated by integrating the relevant peaks in the ^{29}Si spectra and dividing by the number of Si atoms in each species.

The ^{29}Si NMR spectrum of the aqueous phase (Figure 1c) consists of a single peak at a chemical shift (−40.14 ppm) that is lower than the nonhydrolyzed monomer ($\Delta\delta$ = 2.43 ppm). No other significant peaks with similar chemical shifts were identified in the aqueous phase during the 48 h of acid-catalyzed hydrolysis and condensation of MPTMS studied under these conditions. Previously reported studies on the acid-catalyzed hydrolysis of alkoxysilanes at over-stoichiometric water concentrations displayed a rapid and complete hydrolysis of the monomer.[24] Thus, this peak most likely belongs to the fully hydrolyzed monomer (T_0). It is therefore proposed that during the initial hydrolysis of MPTMS in acidic solution,

(22) Rousseau, F.; Poinsignon, C.; Garcia, J.; Popall, M. *Chem. Mater.* **1995**, *7*, 828.

(23) Mazúr, M.; Mlynarik, V.; Valko, M.; Pelikan, P. *Appl. Magn. Reson.* **2000**, *18*, 187.

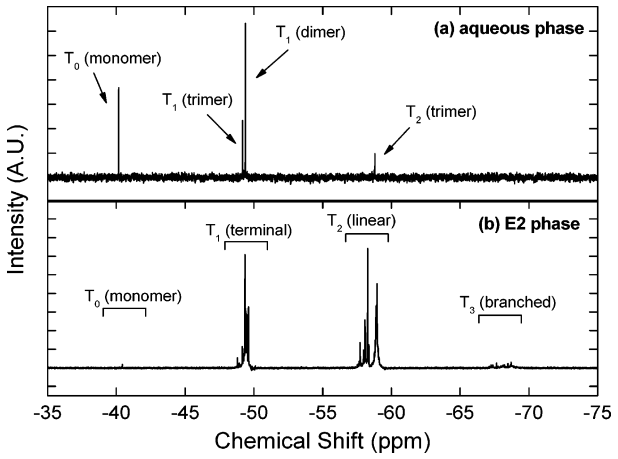

Figure 3. ^{29}Si NMR spectra of (a) aqueous phase and (b) E2 phase after 18 h of acid-catalyzed hydrolysis and condensation. Only three significant species are visible in the aqueous phase (monomer, dimer, and trimer), while the E2 phase contains many different length oligomers with a low degree of cross-linking.

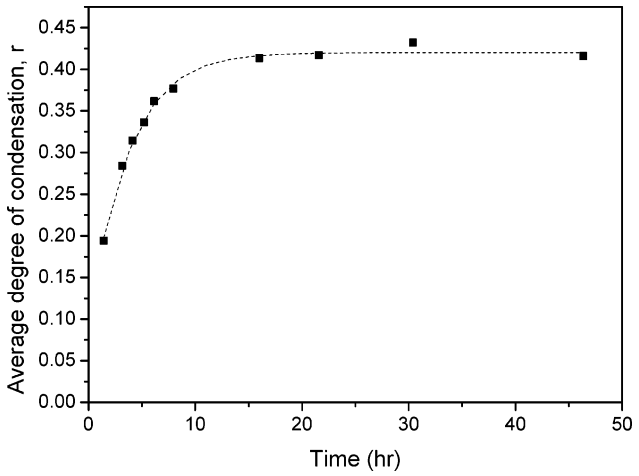

Figure 4. Average degree of condensation, r, for the aqueous phase during acid-catalyzed condensation. The values for r were calculated using eq 1 for the ^{29}Si NMR spectra used in Figure 2.

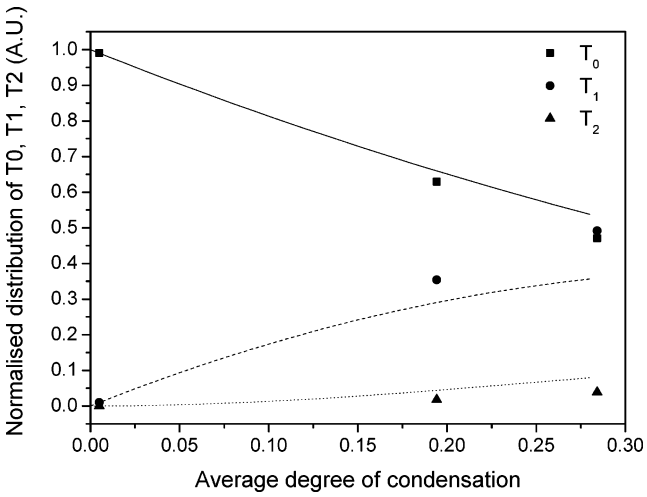

Figure 5. Comparison of the distribution of T_0, T_1, and T_2 species from Figure 2 with the theoretical distribution (solid line, T_0; dashed line, T_1; dotted line, T_2) predicted using Flory–Stockmayer theory for the acid-catalyzed condensation of a trialkoxysilane.

nonhydrolyzed monomer at the E1 phase interface is protonated and subsequently hydrolyzed. The partially hydrolyzed monomer can then transfer into the aqueous phase, where it is rapidly and completely hydrolyzed (Figure 1c) to form a solution or possibly a transparent microemulsion. Nonhydrolyzed monomer was not present in any spectra after 3 h.

The evolution of soluble silica species via acid-catalyzed hydrolysis and condensation is shown in Figure 2. The species were identified by ^{29}Si NMR of the aqueous phase in comparison with previous studies.[18,22,25] Substitution of −OH for the more electron-withdrawing −OSi increases the shielding on the Si atoms and shifts the peaks approximately 9 ppm upfield with each successive condensation step.[25] Dimer (T_1) was thus identified at −49.39 ppm, while linear trimer (T_1 and T_2) was identified at −49.18 ppm and −58.79 ppm, respectively (see Figure 3a). As expected for a linear trimer ($T_1T_2T_1$), the intensity of the trimer T_1 peak was close to double that of the trimer T_2 peak.

The concentration of an oligomer of length n is a balance between reactions involving monomer and oligomer$_{n-1}$ and reactions involving monomer and oligomer$_n$. As there is only a finite initial amount of monomer, the concentration of each oligomer will pass through a maximum when the rate of loss of a given oligomer overtakes its rate of production. If this maximum concentration is greater than the saturation concentration in water for that oligomer, then it will precipitate and form a new phase. The concentration of fully hydrolyzed monomer species passed through its maximum prior to the first measurement, after which it decreased exponentially, while the dimer and trimer species passed through a maximum concentration at ∼4−5 h. This coincided with the development of a new emulsion phase (E2) shortly afterward, which became visible at ∼7.5 h. The initial composition of the E2 phase is unknown; it may be due to a more insoluble longer-chain oligomer, a short-chain oligomer at its saturation concentration, or even a cyclic or branched species. Further condensation must occur within these emulsion droplets, as the viscosity of the E2 phase increases from 100 mPa s after 1 day to 300 mPa s after 5 days (cf. water = 1 mPa s). The E2 phase also has a very low interfacial tension in water (1−2 mN/m) as measured by the pendant drop technique. A similar stability in water by poly(dimethylsiloxane) (PDMS) droplets has been attributed to the presence of linear oligomers at the oil/water interface acting as a surfactant.[26]

The composition of the aqueous and E2 phases after 18 h is shown in Figure 3. The only significant species in the aqueous phase are monomers, dimers, and linear trimers, whereas the E2 phase contains a multitude of different species. The broadness of many of the T_2 and T_1 peaks suggests a mixture of long-chain oligomers. More importantly, it showed the presence of T_3 peaks, which correspond to Si atoms involved in three siloxane bonds, although at a low concentration compared to other Si atoms (7.4% of total Si atoms).

For each spectrum at the times shown in Figure 2, the peak area of each T_n species ($n = 0, 1, 2$, etc.) was integrated and expressed as a relative area compared to the total area of all species.[27] The average degree of condensation,

(24) Brus, J.; Karhan, J.; Kotlik, P. *Collect. Czech. Chem. Commun.* **1996**, *61*, 691.
(25) Brinker, C. J.; Scherer, G. W. In *Sol−Gel Science: The Physics and Chemistry of Sol−Gel Processing*; Brinker, C. J., Scherer, G. W., Eds.; Academic Press: New York, 1990; Chapter 3.
(26) Neumann, B.; Vincent, B. *Langmuir* **2004**, *20*, 4336.
(27) Fyfe, C. A.; Aroca, P. P. *Chem. Mater.* **1995**, *7*, 1800.

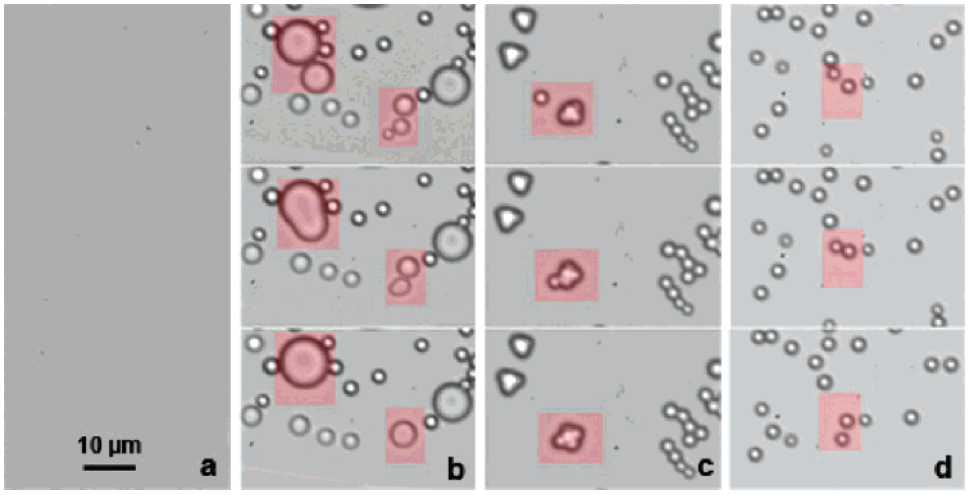

Figure 6. High-speed photographs of the formation and stability of E3 droplets after addition of TEA to an initially clear MPTMS solution: (a) 0 min, (b) 5 min, (c) 12 min, and (d) 20 min.

r, could then be calculated by eq 1:[22]

$$r = {}^1/_2(\%T_1 + 2\%T_2 + 3\%T_3) \quad (1)$$

Figure 4 shows the change in the average degree of condensation in the aqueous phase with time. After 18 h, the average degree of condensation of the aqueous phase remains constant at a value of $r = 0.42$, corresponding to mostly short-chain species. This is in contrast to the average degree of condensation of the E2 phase after 18 h, which has a value of $r = 0.87$, corresponding to mostly long-chain linear species. A low degree of cross-linking is consistent with acid-catalyzed condensation of alkoxysilanes.[19]

Flory−Stockmayer theory also predicts linear condensation under acidic conditions.[28] Its two main assumptions are that all reactive sites have the same reactivity and that there is no cyclization. As the probability of intramolecular reaction is inversely dependent on monomer concentration, the assumption of no cyclization is only valid during the early stages of the reaction, i.e., $r < 0.3$. For a trialkoxysilane, the theoretical size distribution is given by eq 2, where $\%\mathrm{Si}(n)$ is the percentage of Si atoms in an oligomer of length n:[22]

$$\%\mathrm{Si}(n) = 300(2n)!(2r/3)^{n-1}([3 - 2r]/3)^{n+2}(n + 2)!^{-1}(n - 1)!^{-1} \quad (2)$$

The theoretical and experimental distributions of T_0, T_1, and T_2 species are compared in Figure 5. The relative concentration of T_1 species increases more rapidly than predicted, likely due to the lower reactivity of the dimer compared to that of the monomer. This has the subsequent effect of decreasing the relative concentrations of T_0 and T_2 species compared to the theoretical distributions. Nevertheless, it demonstrates the formation of linear chains favored by MPTMS under acidic conditions.

3.2. Base-Catalyzed Condensation and Formation of Organosilica Microspheres. According to the method of Johnston et al.,[17,18] a base catalyst can be added to an acid-catalyzed suspension of MPTMS to promote further cross-linking of the linear chains in the E2 droplets. To investigate whether the particles formed by Johnston et al. could be made more monodisperse by better controlling the reaction conditions, a much lower concentration of base was trialed instead. However, under these conditions it was found that a *new* phase (E3) rapidly formed in the aqueous phase and condensed to produce particles with a narrow size distribution, whereas the E2 droplets did not cross-link at a comparable rate and effectively remained as droplets. Preliminary experiments determined that the average particle size was dependent on the catalyst used (ammonia < ethylamine < trimethylamine < triethylamine), and thus triethylamine (TEA) was used for the remainder of the experiments. A similar reaction mechanism for the base-catalyzed hydrolysis and condensation of dimethyldiethoxysilane (DMDES) in water was postulated by Obey and Vincent;[29] however, polymerization of DMDES can only proceed linearly or by cyclization and, thus, cannot form cross-linked solid particles.

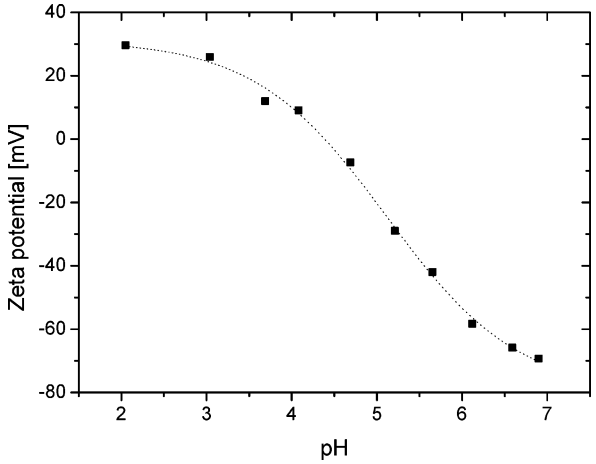

Figure 7. Zeta potential profile of organosilica microspheres for pH < 7. The isoelectric point was measured to occur at pH = 4.4.

The rapid formation of the E3 phase upon addition of a base catalyst was observed using optical microscopy coupled with a high-speed video camera. To avoid possible confusion with any E2 droplets, an aliquot of the acid-catalyzed MPTMS solution was taken after 6.5 h and centrifuged to ensure no E2 droplets were present in the aqueous phase (Figure 6a). Within 30 s of adding TEA, an emulsion rapidly precipitated. Due to the brief nucleation period, the droplets were relatively monodisperse in size.

(28) Klemperer, W. G.; Ramamurthi, S. D. *J. Non-Cryst. Solids* **1990**, *121*, 16.

(29) Obey, T. M.; Vincent, B. *J. Colloid Interface Sci.* **1994**, *163*, 454.

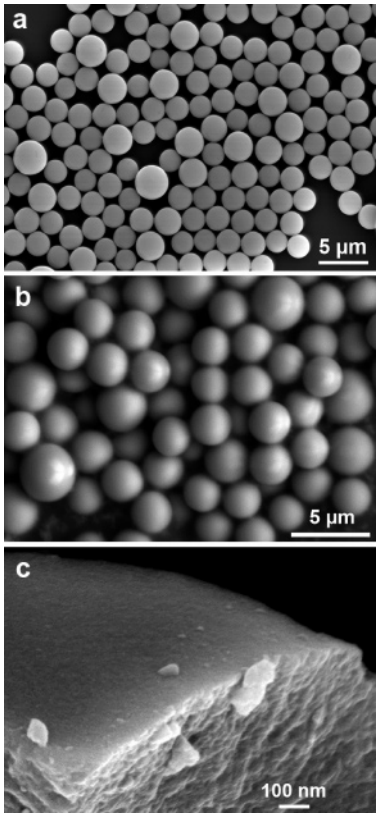

Figure 8. SEM micrographs of organosilica microspheres formed using the method described in Scheme 1 (TEA added after 300 min): (a) SEM image of Pt-coated sample, (b) low-vacuum SEM image of uncoated sample, and (c) high-resolution SEM image of Pt-coated fractured sample.

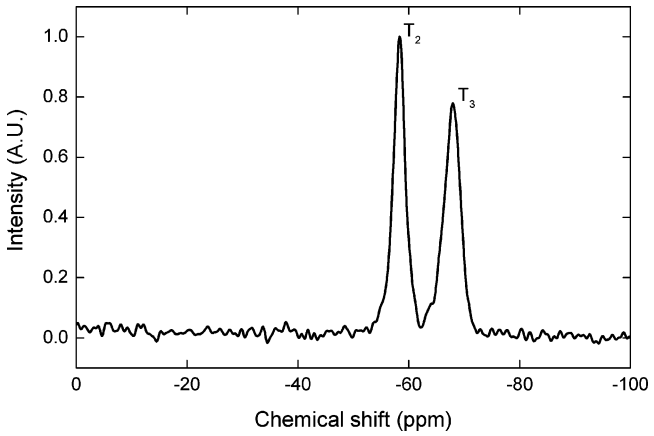

Figure 9. Solid-state ^{29}Si NMR spectrum of organosilica microspheres. Silica species have similar chemical shifts between solution and solid-state NMR. No T_0 or T_1 species were identified ($r = 1.25$).

The series of photographs in Figure 6b−d were obtained by placing an aliquot of the stirred solution onto a microscope slide after different periods of base-catalyzed condensation as indicated in the figure caption. The photographs were intentionally taken near to the boundary of the sample (i.e., at the receding liquid−solid−vapor interface) which promotes coalescence of the emulsion droplets compared to that in the bulk solution. This allowed determination of the time period of base-catalyzed condensation required to form solid particles. It is important to note that the size distribution of droplets in parts b and c of Figure 6 is not representative of the population of droplets under normal bulk conditions.

Table 1. Statistical Results for the Coulter Counter Size Distributions in Figure 10[a]

time (min)	unit particle size (μm)	mean particle size (μm)	size range (μm)	SD (μm)	CV (%)
70	2.90	3.21	1.5−6.1	0.64	19.9
160	2.77	3.13	1.5−6.6	0.72	23.0
300	2.53	3.04	1.5−7.5	0.89	29.3
1100[b]	4.78	4.80	1.4−7.6	1.10	22.9
1100[c]	(∼5.1)	5.29	1.5−8.7	1.29	24.4

[a] The results are representative of 98% of each distribution. Unit particle sizes were determined by the smallest peak in each size distribution. The range covers the minimum and maximum sizes for the representative population. The coefficient of variance (CV) was taken as the standard deviation (SD) divided by the mean. [b] Aqueous phase only. [c] Whole suspension.

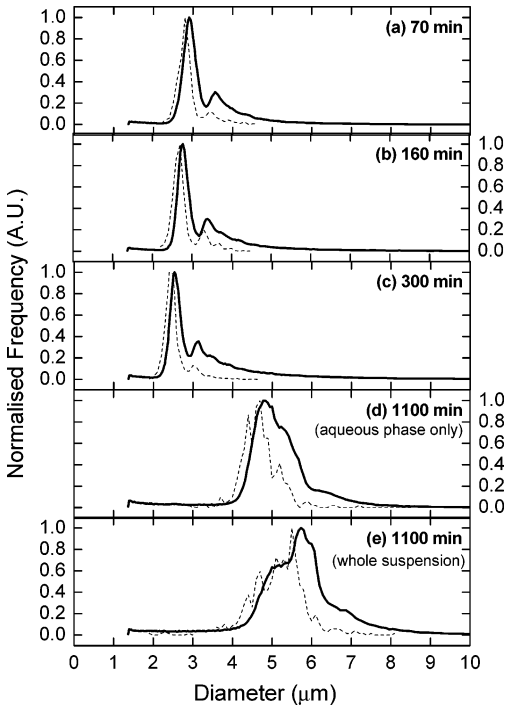

Figure 10. Particle size distributions (solid line, Coulter counter; dashed line, SEM) of organosilica microspheres formed by addition of the base catalyst, TEA, after they had undergone different time periods (70−1100 min) in acid-catalyzed solution.

Five minutes after the addition of TEA, the droplets remained capable of coalescing together, as seen by the sequence of images highlighted in Figure 6b. However, 12 min after the addition of TEA, the droplets have become more condensed and only partially coalesce upon contact (Figure 6c). Finally, 20 min after the addition of TEA, the droplets have become solid particles that can withstand collisions with neighboring particles (Figure 6d). The increase in viscosity of the E3 droplets due to internal cross-linking imparts stability toward coalescence by increasing the interfacial rigidity of the droplets.[30] The reaction is quenched by the addition of an excess amount of ethanol that solubilizes any remaining species or droplets, which can then be removed by multiple centrifugation and washing cycles. Increasing the ethanol fraction beyond 0.5 has previously been found to form a single phase in the base-catalyzed condensation of DMDES,[29] which is in agreement with our observations.

Zeta potential measurements were used to determine the isoelectric point (IEP) for the final particles. Titration

(30) Dowding, P. J.; Goodwin, J. W.; Vincent, B. *Colloids Surf., A* **2001**, *192*, 5.

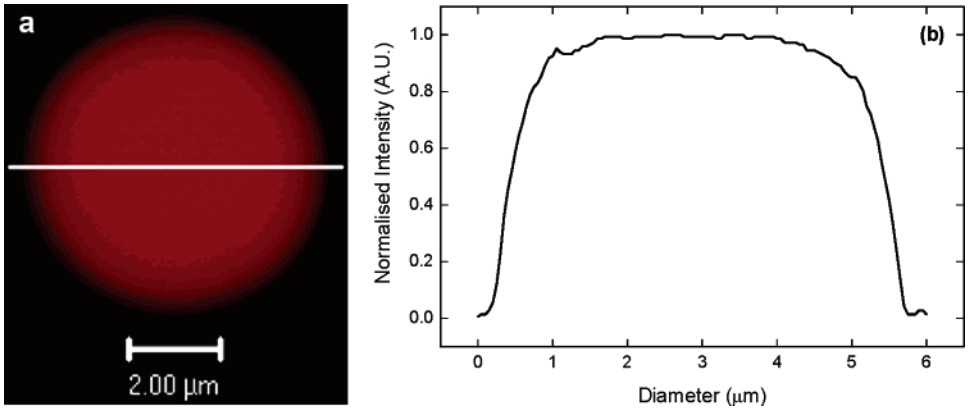

Figure 11. (a) Confocal image of a rhodamine B isothiocyanate labeled organosilica microsphere and (b) normalized fluorescence intensity profile through the center of the microsphere.

with HCl provides a zeta potential profile (Figure 7) which is indicative of the particle surface charge over a broad pH range. In comparison to Stöber silica particles (IEP ≈ 2),[31] the organosilica particles are more basic (IEP = 4.4) due to the presence of mercaptopropyl groups. Similar changes in IEP have been previously reported for basic silica surfaces.[32] In addition, the highly negative zeta potential (∼65 mV) at pH greater than 6 provides an electrostatic barrier to aggregation.

A representative sample (TEA added after 300 min) from the time study described in the Experimental Section was chosen to demonstrate the morphology and particle size distribution. SEM micrographs of these particles are shown in Figure 8. The particle size distribution appears multimodal (Figure 8a), with larger particles likely to be the result of two or more smaller droplets coalescing together at an earlier stage (see Coulter counter results below for further explanation). The external surface of the particles (Figure 8, parts b and c) is smooth and spherical, consistent with an emulsion-based formation, while the interior of the particles appears homogeneous (Figure 8c).

The structural composition of these particles was determined using solid-state ^{29}Si NMR spectroscopy, as shown in Figure 9. Previous studies have found that the chemical shifts of the T_n species are approximately equal between solution and solid-state ^{29}Si NMR,[33] and the peaks have been assigned accordingly. Unlike acid-catalyzed condensation, the majority of Si groups are either branched (T_3) or linear (T_2), with little or no terminal (T_1) or monomer (T_0) present. If 100% condensation is taken to represent the formation of the maximum number of siloxane bonds possible (i.e., $\%T_3 = 100$ and $r = 1.5$), then the ratio of linear to branched groups in Figure 9 indicates that condensation is approximately 83% complete ($r = 1.25$). The absence of terminal (T_1) species suggests that the particles consist of a network of interconnected chains, although isolated cyclic species cannot be ruled out by this alone.

Particle size distributions were obtained to investigate the effects on final particle size due to: (i) different aging times in acid-catalyzed solutions and (ii) the presence of the E2 phase. A comparison of the particle size distributions in Figures 10a−d shows the former effect, while a comparison of parts d and e of Figure 10 shows the latter effect. Particle size distributions determined from SEM and Coulter counter measurements had similar profiles, but SEM distributions were found to be 5−10% smaller in size on average, possibly due to shrinkage caused by drying. The higher proportion of larger particles in the Coulter counter measurements compared to that in the SEM size distributions could also be due to the electrolyte solution required for analysis causing a reduction in the zeta potential of the particles and promoting aggregation.[34] Statistical results from the Coulter counter size distributions are presented in Table 1.

The size distributions after 70, 160, and 300 min have very similar profiles (Figure 10a−c), clearly showing the multimodal nature of the population of particles formed at those times. The narrow peak (full width at half-maximum (fwhm) = 0.35 μm) between 2 and 3 μm represents the unit size of the E3 droplets formed, while peaks at larger sizes represent two or more droplets coalescing together during the first few minutes of the base-catalyzed reaction.

To investigate the effect of the E2 phase on the final particle size distribution, two samples were prepared after 1100 min: the suspension as a whole and the aqueous phase only (separated by centrifugation). TEA was then added to each sample.

The particle size distributions from the two 1100 min samples are provided in Figure 10, parts d and e. The size distribution profile for the aqueous-phase-only sample contains a higher proportion of particles formed by the coalescence of two smaller droplets than the earlier profiles, and the average size of the unit particle is significantly larger. The size distribution of the whole suspension sample is more complex and shows a small increase of the average unit particle size, with an even greater proportion of particles formed by coalescence of two or more droplets.

Importantly, the formation of 4.8 ± 1.1 μm particles in the aqueous phase sample confirms that the E2 phase is not required for formation of the microspheres. Furthermore, the slightly larger particles (5.3 ± 1.3 μm) formed in the whole suspension sample suggests that the E2 droplets act like a reservoir of oligomers that diffuse back into the aqueous phase as the concentration of soluble silica species is decreased by the rapid base-catalyzed condensation reaction.

These results also imply a nonmonotonic relationship between average particle size and reaction time in acid-catalyzed solution. As seen in Table 1, the average size of the unit particle decreases from 2.90 μm (70 min) to 2.53 μm (300 min), before increasing to 4.78 μm (1100 min). The coefficient of variance (CV) of the particles is

(31) Kosmulski, M. *J. Colloid Interface Sci.* **1998**, *208*, 543.
(32) Jesionowski, T. *Colloids Surf., A* **2003**, *222*, 87.
(33) van Blaaderen, A.; Vrij, A. *J. Colloid Interface Sci.* **1993**, *156*, 1.
(34) Schuhmann, R.; Muller, R. H. *Pharm. Ind.* **1998**, *60*, 157.

between 20% and 29%, which is high compared to conventional Stöber synthesis of submicrometer particle sizes (CV = 1−3%),[10] but comparable to those of previously reported syntheses of larger silica microspheres.[14−19]

Finally, confocal microscopy was used to confirm the ability of the functionalized microspheres to covalently bind thiol-reactive dye molecules. Figure 11a shows a thin slice (<0.5 μm) through a representative microsphere after being labeled with rhodamine B isothiocyanate. A normalized fluorescence intensity profile through the center of the microsphere is shown in Figure 11b. Background fluorescence caused by free rhodamine B dye was not detected suggesting that the washing steps were effective in removing excess dye. The uniform intensity across the microsphere indicates that the remaining dye molecules are evenly distributed throughout the interior of the microsphere. This uniform uptake is characteristic of a readily accessible and permeable organosilica network.

4. Conclusions

Thiol-functionalized organosilica microspheres have been synthesized by a novel surfactant-free emulsion-based method. The acid-catalyzed hydrolysis and condensation of the trialkoxysilane precursor, MPTMS, was characterized by ^{29}Si NMR. Over the time period studied, the most significant soluble silica species were monomer, dimer, and trimer, while an insoluble phase developed that consisted of polydisperse droplets of weakly branched long-chain oligomers. The addition of TEA was found to initiate a rapid base-catalyzed condensation reaction that led to the formation of a new insoluble phase. These droplets gradually condensed to produce a multimodal size distribution of functionalized organosilica microspheres. By varying the time period of acid-catalyzed condensation before addition of TEA, microspheres with an average size of 2.5−5 μm have been synthesized. It has also been shown that the thiol-reactive dye, RBITC, can be strongly associated with active thiol sites and evenly distributed throughout the interior of each microsphere. This technique has implications for the production of functionalized solid supports for use in catalysis and biological applications, such as optically encoded carriers for combinatorial synthesis.

Acknowledgment. We thank Lynette Lambert, Associate Professor Justin Cooper-White, Associate Professor Andrew Whittaker, Edeline Wong, Helena Hadisaputra, Christa Pudmenzky, Dr. Kim Sewell, and Angus Johnston for their assistance and expertise. We acknowledge the support of OzNano2Life, which is a project supported by the International Science Linkages program (CG060027). This work was also supported by Nanomics Biosystems Pty Ltd.

LA0514112